

Plans for Kaon Physics at BNL

G. Redlinger^a *

^aPhysics Department, Brookhaven National Laboratory
Upton, New York, USA 11973

I give an overview of current plans for kaon physics at BNL. The program is centered around the rare decay modes $K^+ \rightarrow \pi^+ \nu \bar{\nu}$ and $K_L \rightarrow \pi^0 \nu \bar{\nu}$.

1. INTRODUCTION

There is a long history of kaon physics at the high intensity frontier at the BNL AGS with results going back into the lore of high energy physics. Interest in rare kaon decays at BNL rose anew in the early 1980's with beam intensities starting at 10×10^{12} protons per spill; by the time the program came to an end in 1998, beam intensities were regularly reaching 60×10^{12} protons per spill with a 55% duty cycle. To cite a few "flagship" results, this era produced world-record limits on lepton flavor violating decays such as $K_L \rightarrow \mu^\pm e^\mp$ [1] and $K^+ \rightarrow \pi^+ \mu^+ e^-$ [2], improving limits by 6 and 3 orders of magnitude, respectively. Three orders of magnitude for the decay $K^+ \rightarrow \pi^+ \nu \bar{\nu}$ were covered, resulting in the observation of two events for this mode [3], at a level statistically consistent with Standard Model expectations, but with a central value of the branching ratio tantalizingly high by a factor of about two.

A new era began at BNL in 2000 with the start of the Relativistic Heavy Ion Collider (RHIC) program. The AGS is used as a heavy ion injector to the RHIC ring, but can also be used to accelerate protons in between RHIC fills, allowing a kaon program (for example) to operate concurrently with RHIC at low incremental cost. This kaon program is centered on the rare decays $K^+ \rightarrow \pi^+ \nu \bar{\nu}$ and $K_L \rightarrow \pi^0 \nu \bar{\nu}$ with the corresponding experiments E949 [4] and KOPIO [5].

The literature on the decays $K^+ \rightarrow \pi^+ \nu \bar{\nu}$ and

$K_L \rightarrow \pi^0 \nu \bar{\nu}$ go back over 30 years [6]. For a recent perspective, a good starting point is the review [7]. The physics interest in these decay modes comes from the potential to completely determine the Unitarity Triangle from kaon decays alone. This is shown in Figure 1, which shows the "kaon" unitarity relation $V_{us}^* V_{ud} + V_{cs}^* V_{cd} + V_{ts}^* V_{td} = 0$ or $\lambda_u + \lambda_c + \lambda_t = 0$ where $\lambda_i = V_{is}^* V_{id}$.

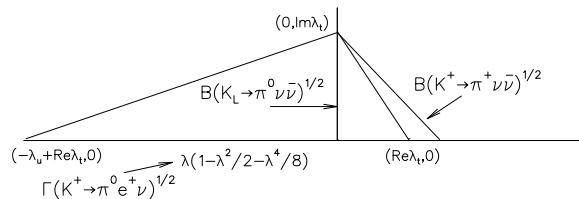


Figure 1. The unitarity triangle determined entirely from kaon decays. The triangle is not drawn to scale; the base is actually about 1000 times longer than the height. From [8].

An inconsistency between the unitarity relation in kaon decays ($s \rightarrow d$ transitions) with that in B decays ($b \rightarrow d$ sector) would be a sign of physics beyond the Standard Model, and precise measurements of the inconsistencies could give some clues to the flavor and CP structure of the new physics. The $K \rightarrow \pi \nu \bar{\nu}$ decay modes are particularly attractive due to the fact that the meson decays can be cleanly related to the short-

*Invited talk presented at HIF04: High Intensity Frontier Workshop, La Biodola, Isola d'Elba, June 5-8, 2004

distance Feynman diagrams at the quark level, allowing a precise extraction of the quark mixing parameters. The theoretical uncertainties in the branching ratios are estimated to be $\sim 7\%$ for $K^+ \rightarrow \pi^+ \nu \bar{\nu}$ and $\sim 2\%$ for $K_L \rightarrow \pi^0 \nu \bar{\nu}$ with an anticipation that the uncertainty for the charged mode could be brought down to $\sim 2\%$ with a NNLO QCD calculation [7]. Promising quantities for comparison include: 1) a comparison of $\text{BR}(K^+ \rightarrow \pi^+ \nu \bar{\nu})$ with the ratio $\Delta m_d / \Delta m_s$ from $B_{d,s}$ mixing, 2) a comparison of the ratio $\text{BR}(K_L \rightarrow \pi^0 \nu \bar{\nu}) / \text{BR}(K^+ \rightarrow \pi^+ \nu \bar{\nu})$ with $\sin 2\beta$ from B_d decays, and 3) a comparison of the Jarlskog invariant [9], proportional to the area of the unitarity triangle, between K and B decays. Experimental challenges include the poor kinematic signature due to the 3-body final state with two neutrinos and the low branching ratio. Current estimates for the charged and neutral modes are $0.78 \pm 0.12 \times 10^{-10}$ and $0.30 \pm 0.06 \times 10^{-10}$, respectively [7], where the quoted uncertainties are dominated by the measurement uncertainties on the parameters of the CKM matrix.

2. E949: $K^+ \rightarrow \pi^+ \nu \bar{\nu}$

Following the observation by E787 of two clean candidates of the decay $K^+ \rightarrow \pi^+ \nu \bar{\nu}$, the E949 experiment was proposed in 1998 to improve the sensitivity by about one order of magnitude. First data were taken in 2002 and first results have been published recently [10].

E949 is based on “modest” upgrades to the E787 apparatus; as such, the background level and signal sensitivity can be predicted with confidence. The experiment uses the entire proton flux from the AGS, increasing the proton intensity from 15×10^{12} per spill to 65×10^{12} ; however, to keep instantaneous rates constant in the detector, the spill length is increased accordingly so we do not gain linearly with proton intensity. The running time per year is increased to ~ 25 weeks, taking advantage of the long RHIC running. Detector upgrades included an addition to the barrel photon veto to increase the number of radiation lengths, better photon veto coverage along the beam direction, higher segmentation of beam tracking elements, improved pion tracking

resolution via changes to the readout electronics of the central drift chamber and range stack straw chambers, improved pion energy resolution by replacing scintillator and by the addition of a phototube gain monitoring system, and finally, upgrades to the trigger/DAQ to handle higher data rates.

2.1. Detector

The E949 detector is shown in Figure 2; most details can be found from the references in [10].

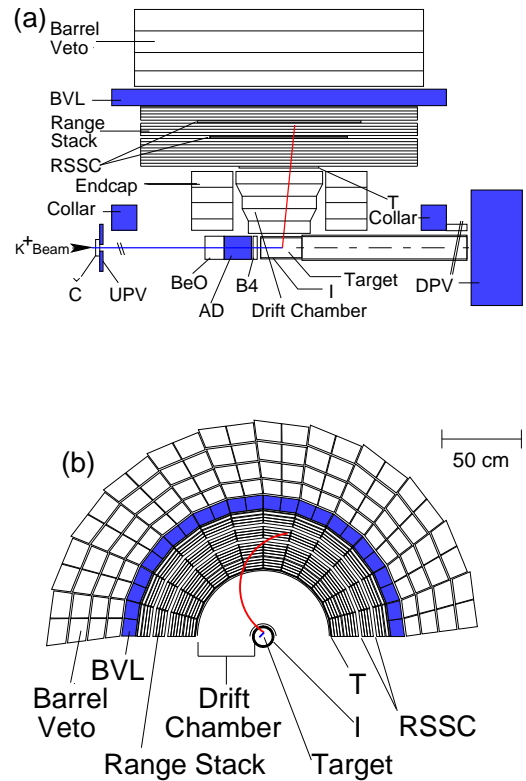


Figure 2. Side (a) and end (b) views of the E949 detector. The detector has cylindrical symmetry; only the top half is shown. Additions to the photon veto system for E949 are shown in blue.

The incoming K^+ beam (K/π ratio ideally

about 4) with a momentum of ~ 700 MeV/c is tracked by Cerenkov counters, MWPCs and scintillator hodoscopes, slowed down in a BeO degrader, and comes to rest in a scintillating fiber target. The stopped kaon technique allows for large geometric acceptance and causes the dominant backgrounds of $K^+ \rightarrow \pi^+\pi^0$ and $K^+ \rightarrow \mu^+\nu$ to appear kinematically as monochromatic peaks, as well as suppressing scattered beam pions. The K decay products are momentum analyzed in a 1T cylindrical field and then stopped in a scintillator “range stack”, allowing measurements of kinetic energy and range to provide redundancy in the kinematics. The $\pi^+ \rightarrow \mu^+ \rightarrow e^+$ decay sequence of the stopped pion is observed by waveform digitizing the scintillator signals, providing a powerful handle against $K^+ \rightarrow \mu^+\nu$ background. Photon detectors surround everything and inactive material in the detector is minimized.

2.2. 2002 run

The proton intensity during the 2002 run was according to design, although it must be said that we did not run concurrently with RHIC. The typical intensity was 65×10^{12} protons in a 2.2 sec spill with a 3.2 sec interspill. Peak intensity reached 76×10^{12} protons/spill. However, there were several non-optimal features of the 2002 run, the first being the short duration, about 12 weeks in total. Next, damage to the primary AGS motor generator set meant running with the backup supply, forcing us to lower the proton momentum to 21.5 GeV with a resulting $\sim 10\%$ loss in K flux; this also resulted in 20% (40%) worse duty factor compared to E787 (E949 proposal). Finally, problems with the beamline separators resulted in a $K : \pi$ ratio of about 2, compared to a typical value of 4 in E787; the resultant instantaneous rates were roughly twice those seen in E787. The integrated kaon flux was about one-third of the total accumulated by E787 over ~ 80 weeks.

2.3. Backgrounds

The main sources of background are the two-body decays $K^+ \rightarrow \mu^+\nu$ ($K_{\mu 2}$) and $K^+ \rightarrow \pi^+\pi^0$ ($K_{\pi 2}$), multibody decays containing muons ($K_{\mu m}$) such as $K^+ \rightarrow \mu^+\nu\gamma$, $K^+ \rightarrow \mu^+\pi^0\nu$, and

$K_{\pi 2}$ with π decay-in-flight, scattered beam pions (either from kaon decay/interaction or pions from the K^+ production target) and K^+ charge exchange (CEX) reactions, resulting in decays $K_L^0 \rightarrow \pi^+l^-\bar{\nu}$, where $l = e$ or μ . To elude rejection, $K_{\mu 2}$ and $K_{\pi 2}$ events have to be reconstructed incorrectly in range, energy and momentum. In addition, any event with a muon has to have its track misidentified as a pion. The most effective weapon here is the waveform digitizer analysis, requiring observation of the $\pi^+ \rightarrow \mu^+ \rightarrow e^+$ decay sequence; this provides a muon rejection factor of about 10^5 . Events with photons, such as $K_{\pi 2}$ decays, are efficiently eliminated by the photon veto; the rejection factor for events with π^0 s is around 10^6 . A scattered beam pion can survive the analysis only by misidentification as a K^+ and if the track is mismeasured as delayed, or if the track is missed entirely by the beam counters after a valid K^+ stopped in the target. CEX background events can survive only if the K_L^0 is produced at low enough energy to remain in the target for at least 2 ns, if there is no visible gap between the beam track and the observed π^+ track, and if the additional charged lepton goes unobserved.

2.4. Offline analysis

The heart of the offline analysis is a robust estimate of the background at the level of a fraction of an event. The key features of the analysis strategy are summarized below.

The sources of background are identified *a priori*, as listed above. The question of backgrounds that may not have been identified in advance will be addressed briefly later.

The same dataset is used for the background studies and signal search. This ensures that the impact on the background estimates of time-dependent effects, intermittent effects (like hardware failures) or intensity-dependent effects are properly taken into account.

The analysis is done blind, meaning that the signal region is hidden (by inverting cuts) while cuts are developed and background levels estimated. The background levels themselves are also estimated in a blind way in order to eliminate bias from cut tuning on the relatively small number

of events left at the end of a typical background study. A uniformly selected subset of the data is used to develop the cuts against the background; the effect of these cuts is then measured (once) in an unbiased way on the remainder of the data.

Two independent cut sets, each with high rejection, are used for each background. These cut sets are played off against each other to measure their background rejection power. For example, for $K_{\pi 2}$ background, the two independent cut sets are the kinematic cuts and the photon veto cuts. By inverting the photon veto cuts (i.e. by demanding the presence of photons), after first removing the non- $K_{\pi 2}$ backgrounds, one can isolate a sample of $K_{\pi 2}$ events from which the kinematic rejection can be measured. And vice versa. The rejection of the two cut sets can be multiplied to give the total rejection if the cuts are not correlated. Ideally the rejections of the two cut sets are comparable so that the rejection of each cut set can be studied with adequate statistics. For the $K_{\mu 2}$ and $K_{\mu m}$ backgrounds, the kinematic cuts are played off against the waveform digitizer cuts. For scattered pions, the delayed coincidence cuts (cuts that ensure that the kaon stopped, then decayed after a suitable time interval) are played off against particle ID cuts in the beamline hodoscopes. For the case where the kaon and pion are from different particles, the delayed coincidence cut can be fooled; for this class of events, cuts on the pattern of hits in the kaon stopping target are played off against cuts that detect multiple tracks in the beamline wire chambers and hodoscopes. The exception to this methodology is the CEX background which is determined largely by Monte Carlo.

Correlations between the independent cuts can spoil the background estimation. We look for explicit evidence for correlations by looking at variations in the rejection of each independent cut as a function of a large set of variables and then seeing if the partner cut shares similar dependences. Problematic regions in cut space are removed by so-called “setup” cuts (more on these in a moment). As a test of the method, the numbers of observed events in regions near the signal region are compared with the predicted background rates based on the product of the rejections of the

independent cut set pairs. The observed consistency gives us confidence that the cuts are independent into the signal region. We also examine all the events that fail only the “setup” cuts to make sure that they are tight enough to remove all correlations; this is also an opportunity to search for hitherto unknown backgrounds since the primary backgrounds have been largely suppressed.

The assessment of candidate events and the computation of the $K^+ \rightarrow \pi^+ \nu \bar{\nu}$ branching ratio are done with a likelihood ratio technique [11]. An event characterization function consisting of a set of discrete bins S_i/b_i describes the relative probability for events occurring in bin i to originate from $K^+ \rightarrow \pi^+ \nu \bar{\nu}$ or background. Here b_i is the expected number of background events from all sources in bin i , and S_i is the expected number of signal events in each bin, given as $\mathcal{B}A_i N_K$ where A_i is the acceptance in bin i and \mathcal{B} is the branching ratio from the fit. Rather than trying to explain the details, let me just state that the validity of the technique was studied extensively and confirmed with Monte Carlo experiments. Reflecting a growing confidence in our ability to predict the background level and a shift in philosophy from “discovery” mode to “measurement” mode, we expanded the E949 pre-determined signal region, letting in more background but also allowing us to gain back about 30% in acceptance. The total background expected in the signal region was 0.30 ± 0.03 events, dominated by $K_{\pi 2}$ background (0.216 ± 0.023). The $K_{\mu 2}$, $K_{\mu m}$, and beam-related backgrounds (including CEX) contributed 0.044 ± 0.010 , 0.024 ± 0.003 , and 0.014 ± 0.003 events, respectively.

After all cuts were applied, one candidate near the $K^+ \rightarrow \pi^+ \nu \bar{\nu}$ endpoint was observed, as shown in Figure 3 (together with the previous data from E787). The estimated probability that the background alone gave rise to this event (or any more signal-like event) was 0.07. At the measured branching ratio (see below), the S_i/b_i for this event was 0.9, compared to values of 50 and 7 for the previous two candidate events seen by E787. The best estimate of the branching ratio, combining data from E787 and E949 is $\mathcal{B}(K^+ \rightarrow \pi^+ \nu \bar{\nu}) = 1.47^{+1.30}_{-0.89} \times 10^{-10}$, consistent

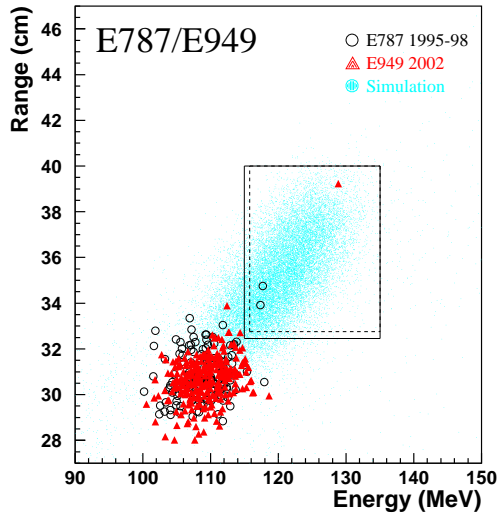


Figure 3. Range (R) vs. energy (E) distribution of events passing all other cuts of the final sample. The circles represent E787 data and the triangles E949 data. The group of events around $E=108$ MeV is due to $K\pi_2$ background. The distribution of $K^+ \rightarrow \pi^+\nu\bar{\nu}$ events from Monte Carlo is shown by dots. The solid (dashed) line box represents the signal region for E949 (E787).

with Standard Model expectations, but intriguing enough to justify completion of the experiment.

3. KOPIO: $K_L \rightarrow \pi^0\nu\bar{\nu}$

The best direct experimental limit on $K_L \rightarrow \pi^0\nu\bar{\nu}$ comes from KTeV [12] where the Dalitz decay of the π^0 was used to locate the K_L decay vertex, reaching a limit $\mathcal{B}(K_L \rightarrow \pi^0\nu\bar{\nu}) < 5.9 \times 10^{-7}$ (90% CL). A model-independent bound (“Grossman-Nir” bound) can be derived [13] from $\mathcal{B}(K^+ \rightarrow \pi^+\nu\bar{\nu})$; with the latest numbers from E949, this leads to a better limit of $\mathcal{B}(K_L \rightarrow \pi^0\nu\bar{\nu}) < 1.4 \times 10^{-9}$ (90% CL). Future searches will all utilize the $\pi^0 \rightarrow \gamma\gamma$ mode. A test of the technique with a narrowly collimated high energy beam (so-called “pencil beam”) was

performed by KTeV [14]. E391a at KEK is the first dedicated experiment to search for $K_L \rightarrow \pi^0\nu\bar{\nu}$ using a pencil beam; data-taking took place this year from February through June. If they can get away with very loose photon veto cuts, they might be able to improve on the Grossman-Nir bound from E949 [15].

KOPIO takes a very different approach. A low energy K_L beam (momentum around 800 MeV/c) is obtained at a 45° production angle. The large angle suppresses hyperon production and the soft neutron spectrum reduces the production of π^0 s from neutron interactions. The “pancake” beam (5mrad vertical vs 100 mrad horizontal) arrives in 200ps-wide microbunches every 40ns, allowing time-of-flight to be used to determine the K_L momentum. The interbunch extinction is expected to be $\sim 10^{-3}$. KOPIO will run with 100×10^{12} protons on target; this requires an AGS injector upgrade. About 3×10^8 K_L are produced per spill, of which about 12% decay in the fiducial volume; these are accompanied by about 3×10^{10} neutrons.

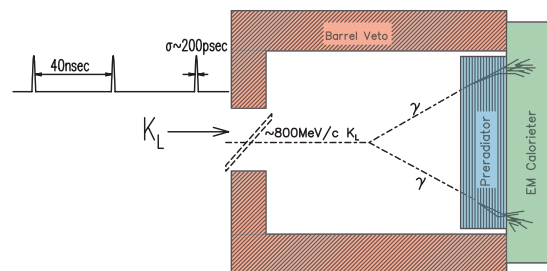


Figure 4. Concept of the KOPIO detector.

The concept is shown in Figure 4. K_L decays are observed in a 4m-long vacuum tank ($\sim 10^{-7}$ Torr) surrounded by scintillator sheets for charged particle vetoing, followed by photon vetoes, using Shashlyk technology [16] in the barrel region and Pb-scintillator “logs” in the upstream wall. The direction of forward photons is

measured in a preradiator consisting of alternating layers of radiator, wire chambers, and scintillator. Together with a constraint from the flat beam, this allows reconstruction of the K_L decay vertex. Photon energies are measured primarily in a Shashlyk calorimeter. The full kinematics of the K_L decay can therefore be determined, suppressing many backgrounds, and serving to relax the photon veto requirements. Furthermore, this provides a second independent cut set (along with the photon or charged veto) and allows a powerful technique for measuring the backgrounds as demonstrated by E787/E949.

3.1. Background suppression

The dominant background is $K_L \rightarrow \pi^0 \pi^0$ with two missed photons. These can be divided into two topologies, one where both photons from one π^0 are missed (“even”) and the other where one photon from each π^0 is missed (“odd”). The power of the kinematic rejection is shown in Figure 5. Cuts on the π^0 energy ($E_{\pi^0}^*$) and on the difference in energy ($|E_{\gamma 1}^* - E_{\gamma 2}^*|$) between the two photons (all measured in the K_L rest frame) are effective.

To fully suppress $K_{\pi 2}$ background, a π^0 detection inefficiency of 10^{-8} is required. E787 obtained a π^0 rejection of 10^{-6} for 200 MeV/c π^0 s which yield photons between 20 and 225 MeV. Inefficiency for single photon detection ranged from about 10^{-2} at 20 MeV down to about 10^{-4} at around 200 MeV. These measurements are currently being redone with the E949 apparatus. To reach 10^{-8} rejection in KOPIO, we take advantage of kinematic handles to reject events with low energy missing photons. The energy of the missing photons can be obtained by subtracting the measured energies of the two observed photons from the K_L energy; requiring significant missing energy suppresses events containing lower energy missing photons. For asymmetric π^0 decays, a cut on the missing mass is effective since the missing mass is proportional to $\sqrt{E_{miss\gamma 1} \cdot E_{miss\gamma 2}}$. The KOPIO goal is to obtain a photon detection inefficiency that is a factor of 3 lower than the E787 measurements; this is thought to be achievable by going to finer sampling (more radiation lengths) for lower (higher)

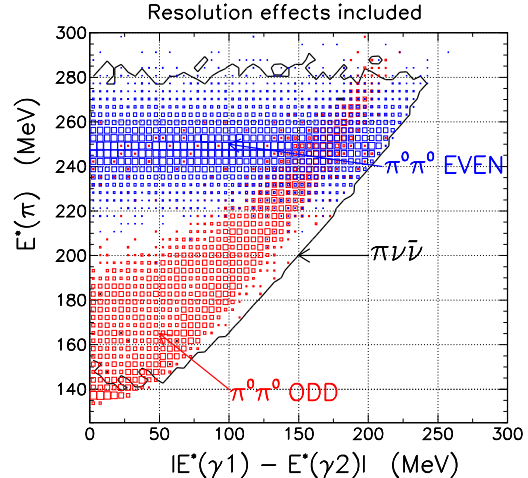


Figure 5. $K_L \rightarrow \pi^0 \pi^0$ background. π^0 energy versus the difference in energy of the two detected photons, measured in the K_L rest frame. The events are shown after a cut on the two photon invariant mass, which constrains the “odd” background to lie on a band.

energy photons. Photons escaping through the downstream beam hole are detected by lead-aerogel Cerenkov counters placed in the downstream section of the beam. The number of photons escaping through the upstream beam hole was found to be negligible.

The $K_{\pi 2}$ “even” background arising from a slow K_L (or neutron) from the previous microbunch can be dealt with by looking at the correlation between $E_{\pi^0}^*$ and the longitudinal π^0 momentum, where $E_{\pi^0}^*$ is calculated assuming that the particle came from the previous microbunch. The background is then cleanly localized whereas the signal is spread out.

To suppress backgrounds containing charged particles, detection inefficiencies for e^-, e^+, π^-, π^+ of better than $10^{-5}, 10^{-4}, 10^{-4}, 10^{-5}$ are required; this seems achievable based on beam tests. The dominant charged-mode background is $K_L \rightarrow \pi^- e^+ \nu \gamma$ where the positron converts asymmetrically before detection in the charged veto, the

low energy γ from the conversion is missed, and the π^- is missed. Cuts on the two photon mass as well as on $E_{\pi_0}^*$ and $|E_{\gamma_1}^* - E_{\gamma_2}^*|$ are effective here as shown in Figure 6.

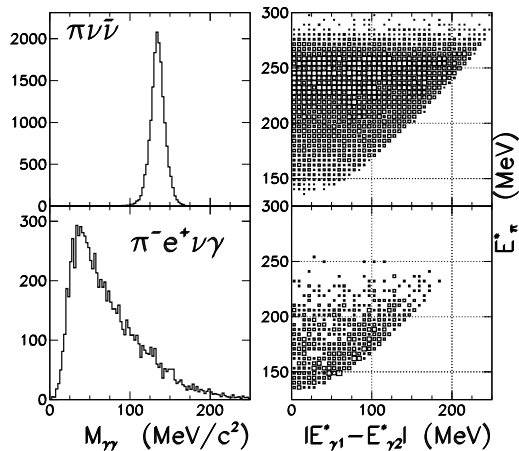


Figure 6. $K_L \rightarrow \pi^- e^+ \nu \gamma$ background. The plots on the left show the two photon invariant mass for signal (top) and background (bottom). The plots on the right show the plane $E_{\pi_0}^*$ vs. $|E_{\gamma_1}^* - E_{\gamma_2}^*|$ for signal and background.

Hyperon decays (primarily Λ) are mostly suppressed by the large angle neutral beam; the production cross section is low and the momentum is low so that all Λ s decay before reaching the fiducial volume. The production of Λ s by interactions of the neutral beam with collimators is reduced by the low momentum; good collimation of the beam and good vertexing ensure that events produced near the last collimator are not a problem. The production of π^0 s from neutron interactions is largely suppressed by having excellent vacuum. The large beam angle also reduces the number of neutrons above π^0 production threshold. The kinematic cuts for K_{π_2} background further suppress the neutrons due to the misassignment of a neutron for an incoming K_L .

A summary of the expected signal and background for the projected 4-year running period of KOPIO is shown in Table 1. Assuming the Standard Model branching ratio, about 40 signal events are expected over a background of 20, leading to a 20% measurement of the branching ratio, or a 10% measurement of $\text{Im}(\lambda_t)$.

Table 1

Expected number of signal and background events assuming the Standard Model branching ratio and 3 years of KOPIO running.

Process	Events
$K_L \rightarrow \pi^0 \nu \bar{\nu}$	40
$K_L \rightarrow \pi^0 \pi^0$	12.4
$K_L \rightarrow \pi^\pm e^\mp \nu \gamma$	4.5
$K_L \rightarrow \pi^+ \pi^- \pi^0$	1.7
$K_L \rightarrow \pi^\pm e^\mp \nu$	0.02
$K_L \rightarrow \gamma \gamma$	0.02
$\Lambda \rightarrow \pi^0 n$	0.01
Interactions ($nN \rightarrow \pi^0 X$)	0.2
Accidentals	0.6
Total background	19.5

3.2. Recent developments

Recent work has concentrated on firming up the detector design.

Studies of the beam include tests of the microbunching width and the interbunch extinction. Measurements in a test run with a 93 MHz RF cavity showed a 240ps width, compared to about 215ps expected from simulation. Using the same simulation to extrapolate to KOPIO running conditions (25 MHz cavity to get the 40ns microbunch spacing and a 100 MHz cavity to get the microbunch width), yields a microbunch width of 185ps so this seems to be in good shape. For the interbunch extinction, a level of about 10^{-3} is needed; the test run with the 93 MHz cavity yielded an extinction of about 0.015. A new test run with a 4.5 MHz cavity was just completed this past June. A \bar{p} beam was used to improve the systematics (previously a photon beam was used). Bunch width and extinction measurements were made in a matrix of RF frequency,

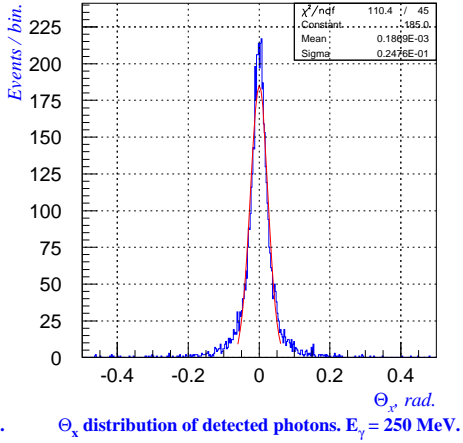


Figure 7. Angular resolution of a preradiator prototype for 250 MeV photons. The fitted sigma is 25 mrad.

RF voltage and $\Delta p/p$; offline analysis and comparisons to simulation are in progress.

The preradiator consists of four $3.5 \times 3.5\text{m}^2$ quadrants (active region $2 \times 2\text{m}^2$). Each quadrant contains 64 layers, where each layer is composed of a sheet of extruded scintillator with wavelength shifting (WLS) fiber readout, wire chamber with cathode strip readout and radiator (copper and aluminum); the thickness of each layer is about $0.03X_0$. The preradiator concept has been tested in a tagged photon beam at the LEGS facility at BNL. The angular resolution for 250 MeV photons is shown in Figure 7. The fitted sigma is 25 mrad. Currently in progress are full-scale prototyping, high voltage and readout electronics, QA studies of the scintillator production facility, and a full mechanical design.

The Shashlyk calorimeter has been extensively studied [17]. It consists of a 48×48 array of modules where each module is $11\text{cm} \times 11\text{cm} \times 65\text{cm}$ in depth, consisting of 300 alternating layers of 0.275mm thick lead and 1.5mm thick scintillator ($16 X_0$). The WLS fibers are read out with an avalanche photodiode (APD). Test beam re-

sults for energy and timing resolution are shown in Figure 8. A fit to the energy resolution yields $\sigma_E/E = (2.9 \pm 0.1)\% / \sqrt{E(\text{GeV})}$. The timing resolution was obtained by looking at the time difference between two Shashlyk modules as a function of the energy in one of the modules. A fit yields $\sigma_t = (90 \pm 10)\text{ps} / \sqrt{E(\text{GeV})}$. Both energy and timing resolution are within the KOPIO specification, and effort has moved on to the full mechanical design, high voltage and readout electronics, and systems for quality control, gain monitoring and cooling of the APDs.

The photon veto system in the barrel region will use essentially the same Shashlyk technology as in the calorimeter, but with 0.5mm/1.5mm lead/scintillator layers, and a total thickness of $17 X_0$. Studies are ongoing to optimize the photon detection efficiency, to understand the mechanical integration with the vacuum tank and to increasing the signal acceptance by taking events where one photon converts in the barrel veto. The upstream wall will consist of “logs” of 1mm/7mm lead/scintillator layers read out with WLS fibers [18]. Light yield, timing and long-term stability tests have been performed on prototypes. Extrapolating to the final design, timing and energy resolutions of $\sim 70\text{ps} / \sqrt{E(\text{GeV})}$ and $5 - 6\% / \sqrt{E(\text{GeV})}$, respectively are expected.

For the charged veto system, the response of plastic scintillator to π^\pm , μ^\pm and e^\pm has been measured in the momentum range of 185-360 MeV/c in a test beam at PSI and compared to simulation. In order to reach a π^- detection inefficiency of better than 10^{-4} in the charged veto system alone, the π^- must be detected before it traverses more than 0.3mm in scintillator and undergoes charge exchange into neutral products; this corresponds to a detection threshold of ~ 75 keV. In reality, some of the neutral products (e.g. photons) will be detected in the photon veto system. In addition, the amount of dead material in front of the veto system must be kept below $20 \text{mg}/\text{cm}^2$; this puts stringent requirements on the membrane separating the high vacuum of the decay volume from the lower vacuum where the charged vetoes will be situated. Current design for the charged veto system in the vacuum tank

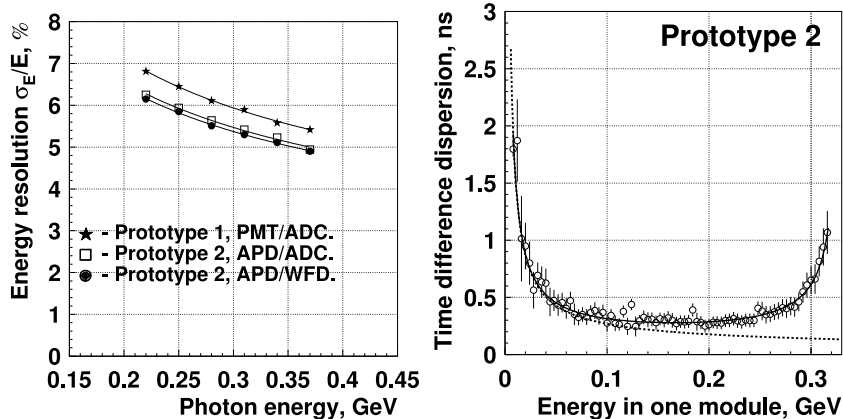


Figure 8. Left: test beam measurements of the energy resolution versus photon energy of the prototype Shashlyk calorimeter. Right: rms of the time difference between two Shashlyk modules versus the energy in one module. The rms rises above 0.3 GeV because there is very little energy deposited in the second module. The time resolution in a single module is shown by the dotted line. From [17].

envisages a single layer of 2mm-thick overlapping sheets of plastic scintillator with direct phototube readout. Tests showed that this approach allows a detection threshold as low as 10 keV and $\pm 5\%$ light collection uniformity over the detector surface. Studies are ongoing on optimizing the thickness, light output, and reflector material as well as on mechanical and vacuum-related issues. In addition, the interplay between the charged and photon vetoes for those cases where the charged particle converts into photons is being studied to optimize the performance of the overall system.

To detect photons passing through the beam hole, an array of lead-aerogel counters (collectively called “catcher”) will be deployed in the beam. The current design calls for a module of 2mm lead, followed by 5cm of aerogel ($n=1.05$) with a flat mirror directing the Cerenkov radiation from the photon conversion to a 5-inch PMT. Around 400 modules will be placed in 25 layers along the beam direction for a thickness of $8.3X_0$ in total. Prototypes have been tested for light yield and for the response to protons (as a substitute for neutrons) and good agreement with simulation was seen. Extrapolating to the final design,

a photon efficiency $> 99\%$ for energy above 300 MeV and a neutron sensitivity of 0.3% for energy around 800 MeV (typical for our beamline) is expected. To cover shower escape from the lateral edges of the catcher for those photons entering at very oblique angles, an array of 2mm/10mm lead-plastic Cerenkov counters (“guard” counter) will be placed in the neutron halo region. Current efforts are directed towards testing of full-scale prototypes, studies of veto blindness by photons (from the production target), neutrons, and K_L decays in the catcher, and estimating rates in the guard counters.

4. Outlook

To clarify the current experimental situation on $K^+ \rightarrow \pi^+ \nu \bar{\nu}$, it would be desirable to complete the E949 program (60 weeks of running in total), but unfortunately AGS operations for HEP were cancelled after the 2002 run. In the meantime, a proposal to complete E949 has been submitted to the NSF. There is good reason to believe that E949 can achieve its design goal if it were to run for the designed length of time; the 2002 run showed that the E949 upgrades worked

and that the backgrounds are well understood. One might even speculate, based on our experience with the higher rates in 2002, that it would be possible to take more instantaneous beam in the future, allowing us to take better advantage of the higher proton intensity being delivered by the AGS. There is also the potential of increasing the sensitivity in the kinematic region below the $K_{\pi 2}$ peak; this region was background limited in E787 analyses [19], including the recently published result on the 1997 data [20], but it is hoped that improvements made in E949 to the photon veto system will make this kinematic region viable. Analysis of the 2002 data in this region is currently in progress. Photon veto improvements in the barrel region have already been verified in the E949 analysis above the $K_{\pi 2}$ peak; what remains to be seen is the (crucial) photon coverage in the beam direction.

While BNL remains firmly committed to E949, experiments have been proposed at other labs to take the sensitivity one step further to the level of between 50 and 100 events. These include decay-in-flight experiments P940 at Fermilab [21], NA48/3 at CERN [22] and a stopped kaon experiment at JPARC [23].

With regards to $K_L \rightarrow \pi^0 \nu \bar{\nu}$, the detector R&D phase of KOPIO is starting to wind down. Key features of the concept have been established, and planning for the construction phase is beginning. The KOPIO project is part of a larger NSF project (“Rare Symmetry Violating Processes”, or RSVP) that includes a search for muon-electron conversion (MECO [24]) at the BNL AGS. RSVP was included in the FY05 President’s Budget for a construction start in 2005; a 5-year construction is envisaged at a cost of about \$140 million, with operations starting in 2008.

5. Acknowledgements

Many thanks to the organizers for a most enjoyable workshop in an incomparable setting. Thanks also to A. Ceccucci for the invitation, and to L. Littenberg and S. Kettell for a careful reading of the manuscript. This work was supported in part under US Department of Energy contract DE-AC02-98CH10886.

REFERENCES

1. A series of results by different experiments, culminating in D. Ambrose *et al.*, Phys. Rev. Lett. 81 (1998) 5734.
2. Again, a series of results by different experiments, the final one from the BNL E865 Collaboration. Publication in progress. A. Sher, Ph.D. dissertation, Universität Zürich (2004).
3. S. Adler *et al.*, Phys. Rev. Lett. 88 (2002) 041803.
4. <http://www.phy.bnl.gov/E949>
5. <http://pubweb.bnl.gov/users/e926/www>
6. For example, M.K. Gaillard and B.W. Lee, Phys. Rev. D (1974) 897, which I believe is the first treatment of rare K decays in the context of electroweak gauge theory.
7. A.J. Buras *et al.*, hep-ph/0405132.
8. A.R. Barker and S.H. Kettell, Ann. Rev. Nucl. Part. Sci. 50 (2000) 249.
9. C. Jarlskog, Phys. Rev. Lett. 55 (1985) 1039.
10. V.V. Anisimovsky *et al.*, Phys. Rev. Lett. 93 (2004) 031801.
11. T. Junk, Nucl. Instr. Meth. A434 (1999) 435.
12. A. Alavi-Harati *et al.*, Phys. Rev. D61 (2000) 072006.
13. Y. Grossman and Y. Nir, Phys. Lett. B398 (1997) 163.
14. J. Adams *et al.*, Phys. Lett. B447 (1999) 240.
15. T.K. Komatsubara, presented at “DAFNE04: Physics at Meson Factories”, Frascati, June 7-11, 2004. To appear in the proceedings.
16. G. Atoyan *et al.*, Nucl. Inst. and Meth. A320 (1992) 144.
17. G. Atoian *et al.*, presented at “Calor 2004”, Perugia, Mar. 29 - Apr. 2, 2004. To appear in the proceedings. Also available at http://pubweb.bnl.gov/people/e926/papers/kopio_papers.html.
18. O. Mineev *et al.*, Nucl. Inst. and Meth. A494 (2002) 362.
19. S. Adler *et al.*, Phys. Lett. B537 (2002) 211.
20. S. Adler *et al.*, hep-ex/0403034. Accepted for publication in Phys. Rev. D.
21. P. Cooper, these proceedings.
22. A. Ceccucci, these proceedings.
23. <http://kaon.kek.jp/~kpwg>
24. <http://meco.ps.uci.edu>